17

Characteristic Conformational Behaviors of Representative Mycolic Acids in the Interfacial Monolayer

Masumi Villeneuve
Graduate School of Science and Engineering, Saitama University
Japan

1. Introduction

Mycobacterial mycolic acid (MA) are long chain 2-alkyl branched, 3-hydroxy fatty acid with two intra-chain groups in the so-called meromycolate chain. On the basis of the nature of the functional groups in the meromycolate chains, MAs are categorized into three major groups: α-MA with no oxygen-containing intra-chain groups, methoxy-MA (MeO-MA) in which the distal group has a methoxy gorup and Keto-MA in which the distal group has a carbonyl group (Fig. 1) (Watanabe et al., 2001; 2002). MAs are characteristic components of mycobacterial cell envelopes, where a major proportion are covalently bonded to the underlying cell wall arabinogalactan (Goren & Brennan, 1979; McNeil et al., 1991; Minnikin, 1982).

In the structural models of the mycobacterial cell envelope proposed previously (Minnikin, 1982; Rastogi, 1991), MAs covalently linked to penta-arabinosyl residues of cell wall arabinogalactan are arranged perpendicular to the cell wall, forming a highly structured monolayer. Recent computer simulation work supported such arrangement of MAs as proposed in the model (Hong & Hopfinger, 2004). This outer leaflet of mycobacterial cell envelope is considered to provide the cells with a special permeability barrier responsible for various physiological and pathogenic features of mycobacterial cells (Daffé et al., 1999). There are various other lipids in the mycobacterial cell envelope and they may also take part in the permeability function of the cell envelope as suggested (Minnikin, 1982; Puech et al., 2001; Rastogi, 1991). Recently, a *Mycobacterium tuberculosis* (*M. tb*) mutant whose MA comprises only α-MA (Dubnau et al., 2000), a recombinant mutant having over-produced MeO-MA with no Keto-MA (Yuan et al., 1998) and a mutant having 40 % less cell wall mycolate (Daffé et al., 1999) have been described. These results show that *M. tb* can be viable with highly modified mycolic acid composition and that its pathogenicity may be related to the types of MAs. Those papers also suggest that MAs on the cell envelope have determining effect on the permeability barrier function of the cell wall outer hydrophobic layer barrier and different MAs may contribute to the cell wall permeability barrier functions in different ways.

In very early studies (Staellberg-Stenhagen & Stenhagen, 1945), the multi-component nature of mycolic acids was not yet known, but it was shown that the total MA formed a stable monolayer on the water surface. It was concluded that MA had extended linear structures, a feature later confirmed by structural analysis (Minnikin, 1982; Minnikin et al., 2002; Rastogi,

1991). Both in the monolayer on the water surface and in the proposed cell envelope lipid structure models, MA is considered to take the same structural arrangement, with the hydrophilic 3-hydroxy and 2-carboxyl groups touching the hydrophilic surface and with the aliphatic chains stretching out in parallel, and normal to the hydrophilic surface. Therefore, detailed studies on the artificial MA layers on water surface should help elucidation of the roles and the nature of actual mycolate layers in the mycobacterial cell envelope.

Recently, limited Langmuir monolayer studies have been performed on a selection of MA (Hasegawa et al., 2000; 2002; Hasegawa & Leblanc, 2003; Hasegawa et al., 2003). Those studies reported that, in a compressed monolayer, α-mycolic acid from *Mycobacterium avium*, apparently took a conformation with three parallel chains, and on further compression, an extended structure, but that the corresponding *M. tb* mycolate appeared to take an extended conformation. As regards the MeO and Keto MAs from *M. tb*, they were reported to take triple chain folded conformations (Hasegawa & Leblanc, 2003; Hasegawa et al., 2003). Regrettably, their monolayer experiments were limited at a single temperature of 25 °C whereas temperature is one of the important factors that influence biological activities of the living cells.

In this chapter, the temperature effect on the Langmuir monolayer packing of all three α-, Keto-, and MeO-MAs from representative slow growing mycobacteria are analyzed to elucidate the conformational behavior of MAs in the monolayer and to understand their roles in the mycobacterial cell envelope.

2. Air/water interface as a biological model membrane

All the biological cells are covered with membranes, through which selective materials are allowed to diffuse in and/or out. It is needless to say that almost all biological activities are intermediated by membranes.

In a real biological membrane system, there always exists specific intermolecular interaction among the membrane-forming components, which is essential for biological activity however sometimes hinders simple understanding of the mechanism. Air/water interface across which dielectric constant changes drastically is a similar self-assembly field to biological interface without particular intermolecular interaction and therefore an ideal model for a biological membrane to study how a certain membrane component behaves there.

Interfacial tension or surface tension, when the interface is between air and water, γ is an essential thermodynamic property for studying interfacial phenomena. A monolayer formed at the air/water interface by a water-insoluble film-forming material is called "Langmuir monolayer." They have been widely studied by using a so-called trough, a shallow container of wide base area equipped with surface tensiometer and a movable barrier for changing the surface area. The performance of amphiphilic molecules such as MAs, lipids, or other biologically significant substance, at interfaces depends not only on the nature of the interface but also strongly on the environmental conditions such as temperature, pressure, pH and so on. Therefore, we studied the temperature effect on the surface tension and the molecular area in the interfacial monolayer of the representative MAs.

3. Structural features of representative mycolic acid samples

The structures of MAs have been characterized (Watanabe et al., 2001; 2002) and MAs are grouped into three major groups, i.e., α-MAs in which X and Y in Fig. 1 are two cyclopropyls or one cyclopropyl and one double bond, MeO-MAs in which X is a methoxy group with a methyl group at the adjacent distal carbon, and Keto-MAs in which X is a keto group with a methyl group at the distal adjacent carbon. In *Mycobacterium avium-intracellulare* complex (MAC), further oxidized wax-ester MA is also known. Further, natural mixtures have both *cis*- and *trans*-cyclopropane rings, the latter having an adjacent methyl group (Fig. 1).

The stereochemistry of the proximal carbon and that of the distal carbon of the *cis*-cyclopropyl group have been determined to be *R* and *S*, respectively, according to the knowedge that the *cis*-cyclopropyl group is derived from the same biosynthetic intermediate of the known stereochemistry (Al Dulayymi et al., 2005). The absolute configurations of the hydroxy-bearing carbon and the carboxyl-bearing carbon in -CH_2-CH(COOH)-CH(OH)-CH_2- are both *R* as reported (Asselineau & Asselineau, 1966; Tocanne & Asselineau, 1968) and as demonstrated by us by easy preparation of its stable chair form acetonide by reduction of MA methyl ester and subsequent acetonide formation (yield 74%).

The non-oxygenated MA samples assayed were so-called type-1 α-MAs (α1-MAs, X and Y both *cis*-cyclopropyls) from *M. tb* (strain Aoyama B), *M. kansasii* (strain 304) and MAC (strain KK41-24) and so-called type-3 α-MAs (α3-MAs), from BCG (strain Tokyo 172) (X *cis*-double bond, Y *cis*-cyclopropyl in Fig. 1) and from MAC (X *cis*-cyclopropyl, Y *cis*-double bond). Their intrachain groups are either *cis*-cyclopropyl or *cis*-double bond but the methylene chain segment lengths vary greatly.

The oxygenated MA samples were type-1 MeO-MA and Keto-MAs from *M. tb* (strain Aoyama B) and *Mycobacterium bovis* BCG (strain Tokyo 172). The structural characteristics and compositions of the MAs studied are summarized in Fig. 1 and Table 1.

4. Experimental details

4.0.0.1 Preparation of the mycolic acid samples

MA samples used in our study were prepared by hydrolysis of purified relevant α-MA, MeO-MA and Keto-MA methyl esters. The procedures for separation and purification of the methyl esters including argentation thin-layer chromatography (TLC) to remove minor components with double bonds and the analytical details are described elsewhere (Watanabe et al., 2001; 2002). Hydrolysis was performed by heating a sealed tube containing MA methyl ester (70 mg), powdered KOH (200 mg) and 2-propanol (2 ml) in an oil bath kept at 80-85 °C for 2 hours with stirring. The hydrolysate was acidified with 2 N H_2SO_4 and treated with hexane, and the mycolic acid obtained was purified by TLC with hexane/AcOEt (4:1, v/v) to remove the byproduct epimer.

4.0.0.2 Other reagents

Distilled reagent grade chloroform (Wako chemicals) was used as the spreading medium. Water was distilled once and deionized by Milli-Q Plus (resistance 18.2 MΩ cm).

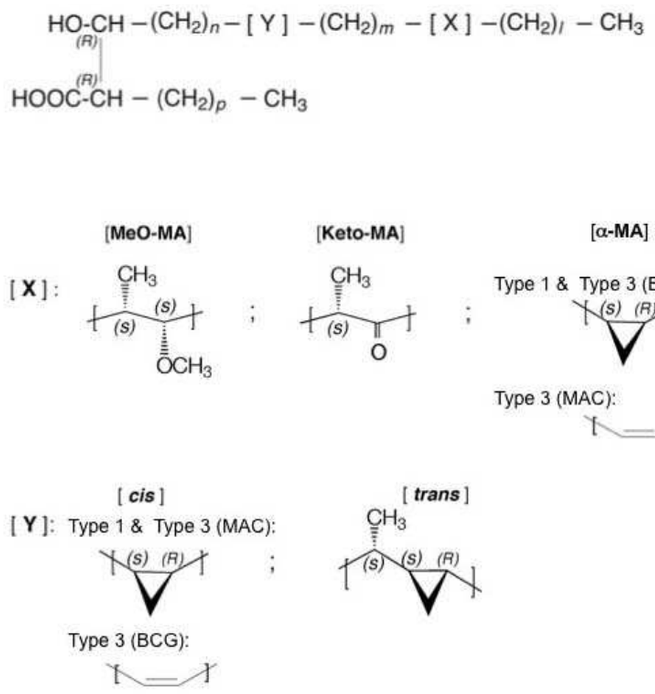

Fig. 1. General structure of MA.

Sample	Origin	Distal group [X]	*p-n-m-l*[a]	*cis* / *trans* ratio of [X][b]
Type 1 *α*	*M. tb*	*cis*-cyclopropyl	23-11-14-19 23-13-14-19	1/0
	M. kansasii	*cis*-cyclopropyl	21-15-14-19 [21-15-16-17 or 21-17-14-17]	1/0.03
	MAC	*cis*-cyclopropyl	21-17-14-17	1/0.14
Type 3 *α*	BCG	*cis*-double bond	23-13-14-19	1/0
	MAC	*cis*-cyclopropyl	21-17-14-17	1/0.14
Type 1 MeO	*M. tb*	*cis*-cyclopropyl	23-17-16-17	1/0.4
		trans-cyclopropyl	23-18-16-17	
	BCG	*cis*-cyclopropy	23-17-16-17	1/0.03
		trans-cyclopropyl	23-18-16-17	
Type 1 Keto	*M. tb*	*cis*-cyclopropyl	23-15-18-17	1/0.4
		trans-cyclopropyl	23-16-18-17	
	BCG	*cis*-cyclopropyl	23-15-18-17 23-17-18-17	1/0.33
		trans-cyclopropyl	23-16-18-17	

a. Values of major components.
b. Ratios implied by ^{1}H-NMR spectra.

Table 1. Structural features of the MA samples.

4.0.0.3 Surface pressure vs. mean molecular surface area (π vs. A) isotherms measurement

The Langmuir monolayers were prepared by spreading a chloroform solution of MA (1 ml, ca. 6×10^{-5} M) on the water surface. Surface pressure (π) vs. mean molecular area (A) isotherms of the Langmuir monolayer of MA spread on water were measured by a Lauda film balance (FW1). Here, π is defined as $\pi = \gamma^0 - \gamma$, where γ^0 is the surface tension of water with no monolayer. The area of the water surface was about 562 cm^2 in this trough. The compression rate of the monolayer was 14 $Å^2$ $molecule^{-1}$ min^{-1}. π vs. A isotherms were measured at various temperatures in the range of $10 \sim 46$ °C. The subphase temperature was controlled within the accuracy of ± 0.2 °C. The room temperature was thermostatted at 23 ± 1 °C. Each measurement was repeated 3∼5 times.

4.0.0.4 Ellipsometry:

Ellipsometry (Tompkins & McGahan, 1999) was performed on a Nanofilm EP^3 (NFT Co., Göttingen, Germany) with a home-built trough installed on the stage. The trough was thermostatted at the temperatures as specified in Table 2 (error within $\pm$ 0.2 °C). The monolayer was prepared and compressed with a Teflon-coated barrier to the target π values. The refractive index was taken to be 1.48 in evaluation of monolayer thickness.

5. Conformational behavior of MAs in the monolayer

The behavior of MAs in the interfacial monolayer is most effectively shown by phase diagram of the monolayer. The phase diagrams are constructed by plotting the surface pressures at the bends on the π vs. A isotherms which correspond to the phase transitions π^{tr} and to film collapsing π^{cp} against the temperature (Villeneuve et al., 2005; 2007; 2010). As they will be shown later, at low temperature (T) and low surface pressure (π: defined as the decrement of surface tension due to monolayer formation), all these MAs form a condensed four-chain (so called W-shape) structure in which the 2-alkyl side chain and the three methylene-chain segments are parallel to each other. The two functional groups appear to allow the meromycolate chain to fold up into a compact parallel arrangement. As T and π are increased, α- and MeO-MAs tend to take stretchedout structures in which the distal functional group in the meromycolate chain leaves the near-hydroxy group location. The conformation of Keto-MA is little affected by the changes in T and π and the four-chain form is retained.

5.1 α-MA monolayers

The phase diagrams (π vs. T diamgram), where surface pressure of phase transition π^{tr} and that of film collapse π^{cp} are plotted against T and the diagram where mean molecular areas at π^{tr} and π^{cp} are plotted against T are shown in Figs. 2-6. Those diagrams, some of which are quite simple and others more complex, demonstrate that π^{tr}, π^{cp}, A^{tr} and A^{cp} all changed depending on the temperature. As shown, all those diagrams for the present α-MAs from different origins gave analogous features: In Figs 2a, 3a, 4a, 5a and 6a, each of the π^{cp} vs. T diagram gave a cusp in the range of $32 \sim 39$ °C. The T at the cusp were different in different samples, and at that point, A^{cp} vs. T curve was discontinuous, as shown in Figs. 2b, 3b and 4b, though it is not quite obvious in Figs. 5b and 6b. One characteristic feature noted in those diagrams is that the π^{cp} values of *M. tb* complex α-MAs, such as α1-MA from *M. tb* and α3-MA from BCG were much higher, and accordingly the A^{cp} values much smaller than the

corresponding values of α1-MAs from *M. kansasii* and MAC. At the temperature just below the cusp in the range of 32 ∼ 39 °C, the π^{cp} values for *M. tb* α1-MA, BCG α3-MA, *M. kansasii* α1-MA and MAC α1-MA were 60, 58, 42 and 34 mN m^{-1}, respectively, and the A^{cp} values were 36, 36, 43 and 41 $Å^2$ $molecule^{-1}$, respectively.

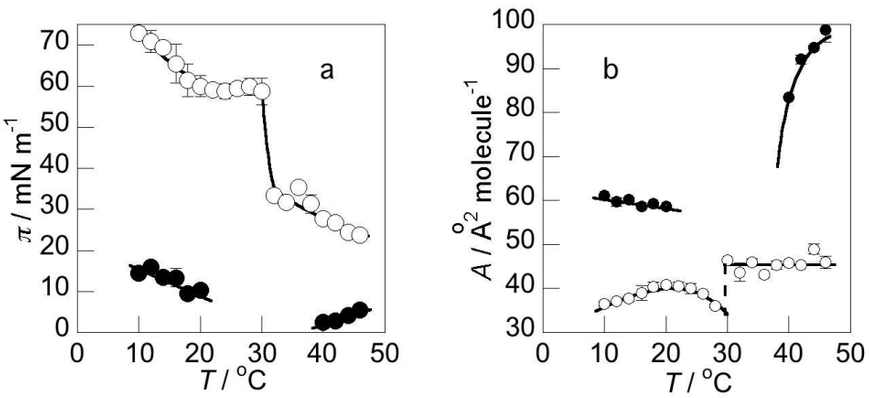

Fig. 2. (a) Phase diagram and (b) A^{cp}, A^{tr} vs. T curves of *M. tb* α1-MA. (—◯—) film collapse; (—●—) phase transition.

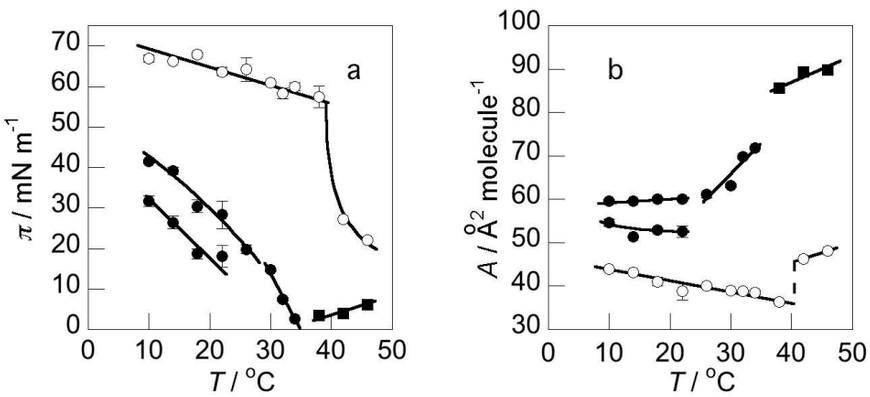

Fig. 3. (a) Phase diagram and (b) A^{cp}, A^{tr} vs. T curves of BCG α3-MA. (—◯—) film collapse; (filled symbols) phase transition.

All the phase diagrams of the α-MAs in the present study, having varied hydrocarbon segment lengths and different X and Y combinations (Fig. 1), showed the same features. As the surface pressure was increased by compression, the molecules apparently changed from the 4-chain W-shapes to extended ones, having a mean molecular area corresponding to that of two hydrocarbon chains. As described in the literature (Villeneuve et al., 2010), when no restriction is applied, the W-shape conformation obtained by Monte Carlo (MC) calculation retains its form during a series of 2.5 ps molecular dynamics (MD) runs, suggesting that the sparsely scattered α-MA molecules on the water surface are in the W-shape before compression is started. When the film is compressed, in a very low surface pressure and low temperature region of the phase diagram the first phase-transition point appears on the π vs. A isotherms, where the original condensed phase changes to another condensed phase. In the A^{cp}, A^{tr} vs. T diagrams, when the temperature is between 10 °C and 20 °C, the A^{tr} values remain more or less at around 60 $Å^2$ $molecule^{-1}$, which shows that at that stage the molecules are in W-shape. At this first phase-transition point, the molecules of W-shaped conformation is

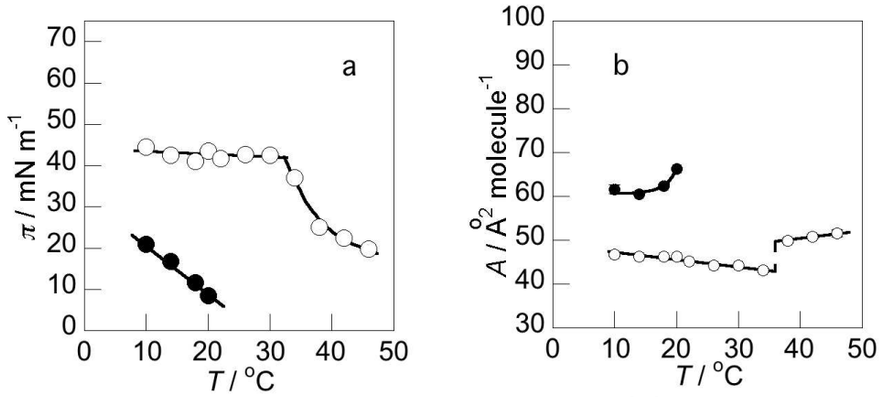

Fig. 4. (a) Phase diagram and (b) A^{cp}, A^{tr} vs. T curves of *M. kansasii* α1-MA. (—◯—) film collapse; (—●—) phase transition.

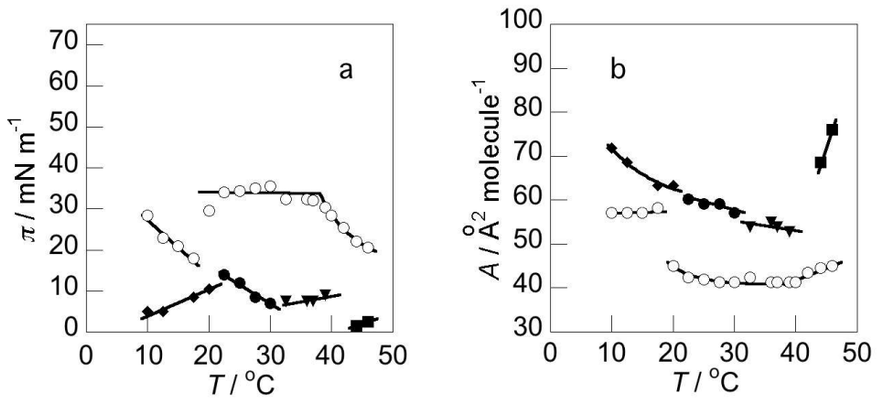

Fig. 5. (a) Phase diagram and (b) A^{cp}, A^{tr} vs. T curves of MAC α1-MA. (—◯—) film collapse; (filled symbols) phase transition.

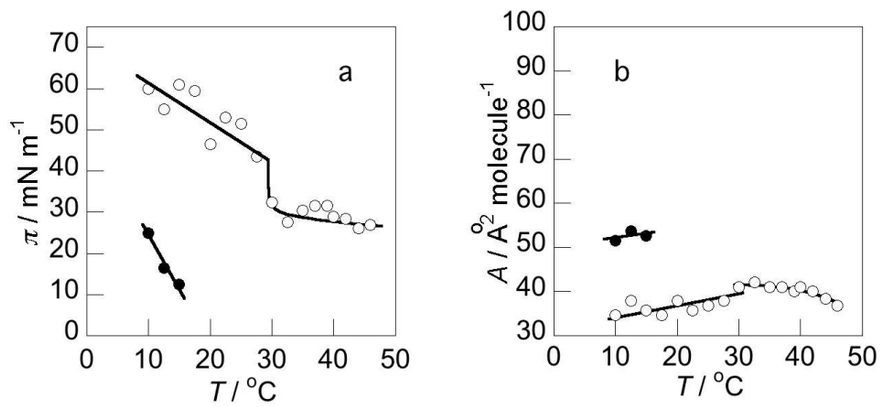

Fig. 6. (a) Phase diagram and (b) A^{cp}, A^{tr} vs. T curves of MAC α3-MA. (—◯—) film collapse; (—●—) phase transition.

considered to start unfolding, thereby inducing conversion of the *trans* form to the *gauche* form, which then start extending. The geometry change should be facile, because DFT calculations demonstrated a very small energy barrier between the two geometries and the

sharp NMR signals of the relevant atoms implied that the conversion between the two should take place easily. Though an exothermic transition is noted in the phase diagrams, the π^{tr} values tend to decrease generally in the π vs. T diagrams as the temperature increases, which means that the transition taking place at the surface pressure is endothermic. This also implies that the conversion from *trans* to *gauche* geometry takes place during this phase transition. The decrease in the π^{tr} values, however, is not so marked as in the case of MeO-MA (Villeneuve et al., 2007) as will be shown below, probably because the change in the conformation of α-MAs does not involve breaking of hydrogen bonding.

Elasticity and fluidity of the biological membranes are important factors in relation to their functions. The elasticity modulus

$$E = -A(\partial\pi/\partial A)_{T,p} \tag{1}$$

or E values of α-MAs are in the range of 80 to 200 mN m^{-1}, which roughly correspond to the values of liquid condensed film of common fatty acids, such as stearic acid (Villeneuve et al., 2005). When π is 10 mN m^{-1} and T below 20 °C, where the molecules are considered to be taking the W-shape according to the phase diagrams, the E values of those MAs are equivalent to those at higher temperatures where the molecules are in extended conformations. Thus, α-MA forms a monolayer which is fluid in whatever conformation the α-MAs might be taking and in which the α-MAs is ready to change the molecular area in response to outside pressure and temperatures.

5.2 Keto-MA monolayers

The phase diagrams of Langmuir monolayer and the A^{cp}, A^{tr} vs. T diagrams for Keto-MAs are quite different from those for α-MAs as shown in Fig. 7. The phase diagrams for Keto-MAs are much simpler than those for the α-MAs and the values of A^{cp} are much larger for the Keto-MAs than for the α-MAs. Keto-MA forms a condensed monolayer more rigid than a liquid condensed film but less stiff than a solid condensed film over a wide range of temperature and surface pressure. A^{cp} of Keto-MA is shown to be about 80 Å^2 molecule^{-1}. Moreover, the monolayer is in a condensed state as indicated by the elastic modulus, e.g., about $E = 1000$ mN m^{-1} for *M. tb* and about $E = 300$ mN m^{-1} for BCG. Accordingly, it seems reasonable to assume that in the Keto-MA molecules the meromycolate chain bends at the cyclopropane and at the carbonyl group to form a 4-chain structure whose four hydrocarbons are packed tightly in parallel, with the carbonyl group touching the water surface and hydrated.

5.3 MeO-MA monolayers

The phase diagrams of monolayer and the mean molecular area vs. T diagrams for MeO-MAs from *M. tb* and BCG are shown in Fig. 8. In each of the phase diagram, a characteristic phase transition is shown, of which surface pressure greatly decreased with an increase in temperature. This phase transition is reversible as has been confirmed by repeated compression-expansion measurement of the π vs. A isotherm. A^{tr} takes values from 70 to 90 Å^2 molecule^{-1} for *M. tb* and from 70 to 110 Å^2 molecule^{-1} for BCG*. Even with such large mean molecular areas, the monolayers are in condensed states. For example the elastic moduli below π^{tr} of the two MA samples are $E = 100 \sim 350$ mN m^{-1}. On the other hand, A^{cp} takes values less than 60 Å^2 molecule^{-1} down to 38 Å^2 molecule^{-1} for both MeO-MA samples*.

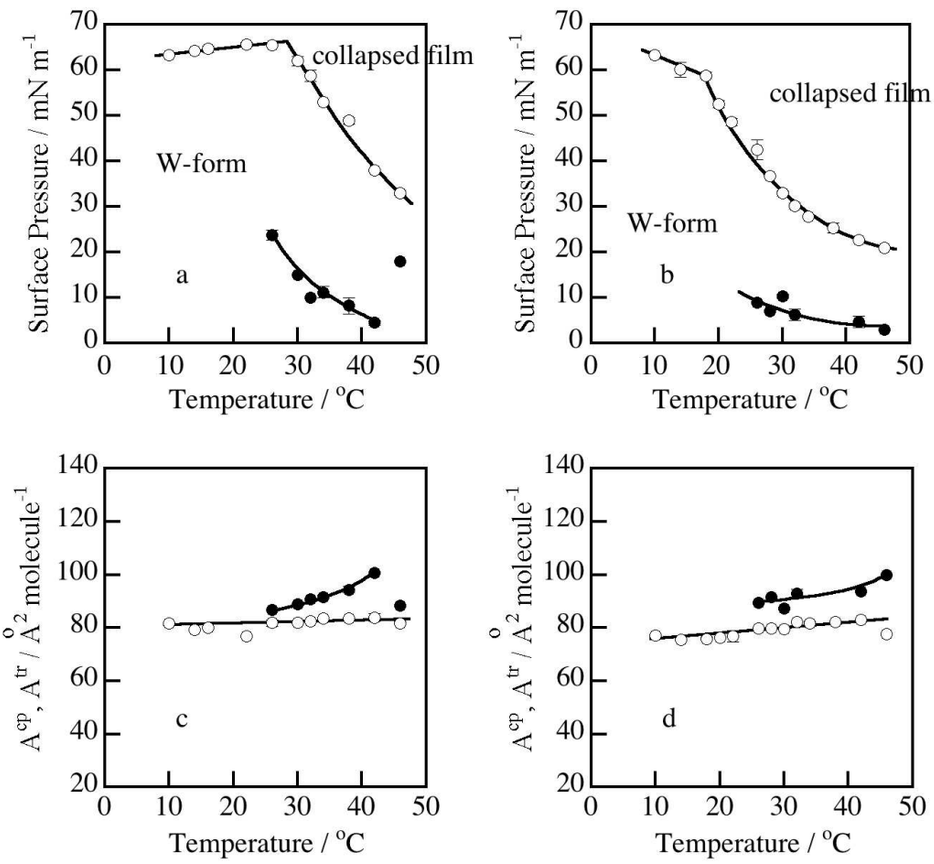

Fig. 7. Phase diagrams and A^{cp}, A^{tr} vs. T curves of Keto-MAs. (a) Phase diagrams for *M. tb* Keto-MA; (b) BCG Keto-MA; (c)A^{cp}, A^{tr} vs. T diagrams for *M. tb* Keto-MA; (d) BCG Keto-MA; (—○—) film collapse; (—●—) phase transition.

These results strongly suggest that MeO-MAs take W-shaped conformations under low T and low π condition.

Enthalpy changes associated with these phase transitions are tentatively (because the systems consist of known and unknown species) evaluated by applying the Clausius-Clapeyron equation derived for insoluble monolayer to the π^{tr} vs. T and A^{tr}, A^{cp} vs. T curves (Motomura, 1967).

$$\left(\frac{\partial \pi^{tr}}{\partial T}\right)_p = \frac{1}{T}\frac{\Delta_l^s h}{\Delta_l^s A}, \tag{2}$$

where

$$\Delta_l^s h = h_{fs} - h_{fl} \tag{3}$$

$$\Delta_l^s A = A_{fs} - A_{fl} \tag{4}$$

Here, h_{fl} and h_{fs} are the partial molar enthalpies, and A_{fl} and A_{fs} are the areas per mole at equilibrium, in different states. Here, the more condensed state is denoted by 's'. The values of A^{tr} and A^{cp} are employed as A_{fl} and A_{fs} for evaluation of $\Delta_l^s A$. The results are shown in Fig. 9 together with the values of enthalpy change associated with the phase transition

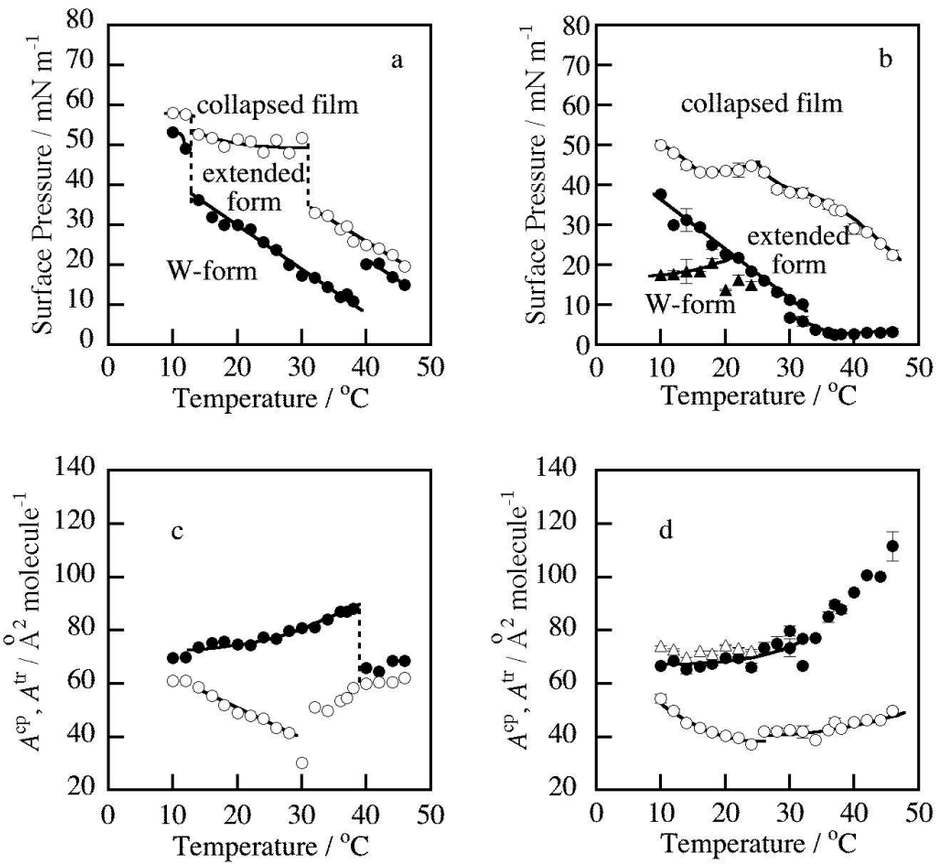

Fig. 8. Phase diagrams and A^{cp}, A^{tr} vs. T curves of MeO-MAs. (a) Phase diagrams for *M. tb* MeO-MA; (b) BCG MeO-MA; (c)A^{cp}, A^{tr} vs. T diagrams for *M. tb* MeO-MA; (d) BCG MeO-MA; (open circle) film collapse; (filled symbols) phase transition.

observed in the low temperature and low surface pressure region of the phase diagrams for *M. tb* α1-MA (Fig. 2a) and BCG α3-MA (Fig. 3a).

In the entire temperature range, the $\Delta_l^s h$ values for the MeO-MAs are larger than those for the α-MAs. This is probably because the methoxy group is hydrated in the interfacial layer and when the MeO-MA transforms to an extended conformation, hydrogen bondings must be broken.

One possible reason that may explain the difference in the behavior of the MAs is the difference in the hydrophilic nature of the functional group [X]. The adhesion energy of hydrophilic groups to water surface such as ether, ketone and alcohol groups is said to be fairly independent of other parts of the molecule and at 20 °C, those of diisopropyl ketone and of diamyl ether are reported to be 74 and 68 mJ m^{-2}, respectively (Timmons & Zisman, 1968). The difference may not be much, but may play some role in the conformational behaviors of MeO- and Keto-MAs in the water surface monolayers. α-MAs having no hydrophilic group at the [X]-position may be more free to take a stretched-out structure, even at a lower surface pressure.

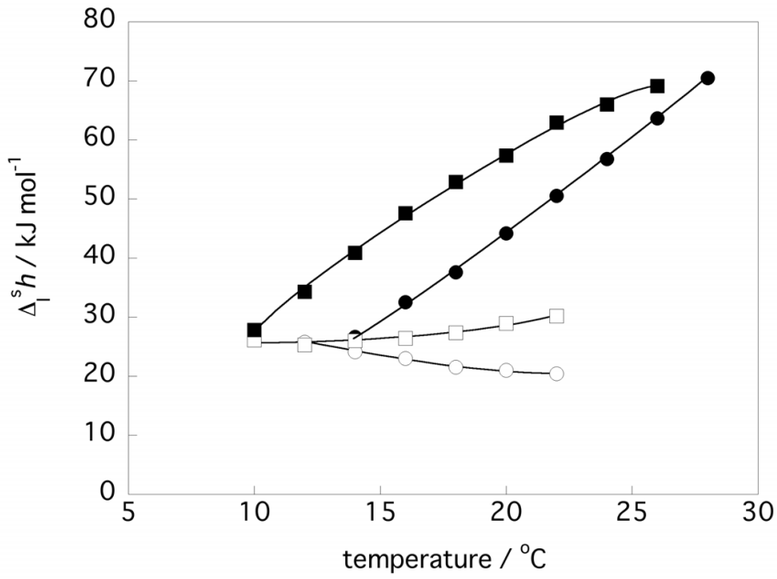

Fig. 9. Enthalpy change associated with phase transition. *M. tb* α 1-MA (—◯—); *M. tb* MeO-MA (—●—); BCG α 3-MA (—□—); BCG MeO-MA (—■—).

* The A^{tr} and A^{cp} must be corrected to the values mentioned here from the ones reported in the literature (Villeneuve et al., 2007).

5.4 Other data supporting conformational behavior of Keto- and MeO-MAs deduced from the monolayer study

5.4.0.5 Ellipsometry

Conformational transition from a 4-chain structure to an extended one suggested from the π vs. A study is supported by the *in-situ* ellipsometry. Results of the ellipsometric measurement are summarized in Table 2. Thus the thickness of the monolayer of MeO-MA at $T = 32$ °C and $\pi = 30$ mN m^{-1} is larger by a factor of $1.7 \sim 2$ than that of MeO-MA at $T = 18$ °C and $\pi = 18$ mN m^{-1} and those of Keto-MA at $T = 18$ °C and $\pi = 30$ mN m^{-1} and $T = 32$ °C and $\pi = 20$ mN m^{-1}. The thickness of MeO-MA monolayer changes from 2.91 nm for *M. tb* and 2.78 nm for BCG at $T = 18$ °C and $\pi = 18$ mN m^{-1}, which is almost the same value with the thickness of Keto-MA, drastically to 4.96 nm (*M. tb*) and 5.62 nm (BCG) at $T = 32$ °C and $\pi = 30$ mN m^{-1}. As for Keto-MA whose A^{cp} values imply that its carbonyl group is hydrated at the water surface to give a four-chain molecular conformation, the monolayer thickness is unchanged irrespective of the surface pressure or temperature (Table 2).

Origin	Keto-MA			MeO-MA		
	T / °C	π / mN m^{-1}	thickness / nm	T / °C	π /mN m^{-1}	thickness / nm
M. tb	18	30	2.90 ± 0.07	18	18	2.91 ± 0.05
				32	30	4.96 ± 0.88
BCG	18	30	2.90 ± 0.05	18	18	2.78 ± 0.04
	32	20	2.80 ± 0.08	32	30	5.62 ± 0.18

Table 2. Thickness of Langmuir monolayer estimated by ellipsometry.

5.4.0.6 Computer simulation

The MAs subjected to MC calculations and MD simulations were *cis*-cyclopropyl MeO-MA with *n-m-l* of 17-16-17, *trans*-cyclopropyl MeO-MA with *n-m-l* of 18-16-17, *cis*-cyclopropyl Keto-MA with *n-m-l* of 15-18-17 and 17-18-17 and *trans*-cyclopropyl Keto-MA with *n-m-l* of 16-18-17 (Table 1). The structural models of MeO- and Keto-MA produced by MC calculations were all of 4-chain structure as illustrated in Figs. 10a and b. The fact suggests that this type of arrangement of carbon chain segments is appropriate for energetically stable conformations. After the molecular dynamics (MD) simulation, Keto-MA having 4-chain structure normally retained the original 4-chain form (Fig. 10e) and seldom gave extended structures. On the other hand, MeO-MA, whose starting structure is as in Figs. 10a and b, often gave extended structures (Fig. 10c), though some models retained 4-chain structures as seen in Fig. d (Villeneuve et al., 2007).

Intra-molecular hydrogen bonding involving either the oxo or methoxy group and the 3-hydroxy carboxylic acid group may contribute to some extent to the retaining of the 4-chain structure. However, one of the major causes for the difference observed in the results of MD simulation of the two types of MAs seems to be in the difference in the lengths of the methylene chain segments or in the *n-m-l* values. As described previously (Watanabe et al., 2002), the major component of the MeO-MA is *cis*-cyclopropyl-containing MeO-MA acid with the *n-m-l* value of 17-16-17, and the minor component with a *trans*-cyclopropane with the *n-m-l* value of 18-16-17. In those MeO-MAs, n is larger than m. In the starting models for MD of MeO-MA, having the energetically stabilized 4-chain structure produced by MC (Figs. 10a and b), a bulky group consisting of a methoxy group and the adjacent methyl group is at a position to obstruct the compact arrangement of the 4 chains, as demonstrated by the molecular minimized energy levels: for the models in the literature (Villeneuve et al., 2007), the minimized energy levels of *cis*- and *trans*-MeO-MAs are $-13 \sim -19$ kcal mol^{-1} and $-7 \sim -12$ kcal mol^{-1}, respectively, whereas those of *cis*- and *trans*-Keto-MAs are $-24 \sim -32$ kcal mol^{-1} and $-28 \sim -38$ kcal mol^{-1}. The vibrations of the bulky group locating at or above the location of the 3-hydroxy carboxylate group during MD simulation may disturb the neat arrangement of the neighbouring chains to induce faster and more efficient deviation from the original 4-chain structure. In Keto-MA, the *n-m-l* value for the major *cis*-cyclopropane containing component is 15-18-17 or 17-18-17 and that for the major *trans*-cyclopropane containing component is 16-18-17, n being smaller than m. Thus, the oxo and the adjacent methyl groups are normally at the end or stretching out of the square pillar-like 4-chain structure. It allows a more compact solid arrangement of the methylene chains in the molecule and the more quiet vibration of the alpha-methyl oxo group may tend to be less disturbing for the 4-chain arrangement during the MD.

The fact that the oxo group is normally situating at the end or out of the 4-chain pillar structure may contribute to the more stable 4-chain structure of Keto-MA in Langmuir monolayers; it assures that the oxo group touches and bonds to the water surface firmly. On the other hand, in MeO-MA, the methoxy group may often be above the level of the location of the carboxyl group, which touches the water surface. Therefore, although the hydrophilicity of the methoxy group approaches that of an oxo group, the methoxy group may not be able to interact decisively with the water surface.

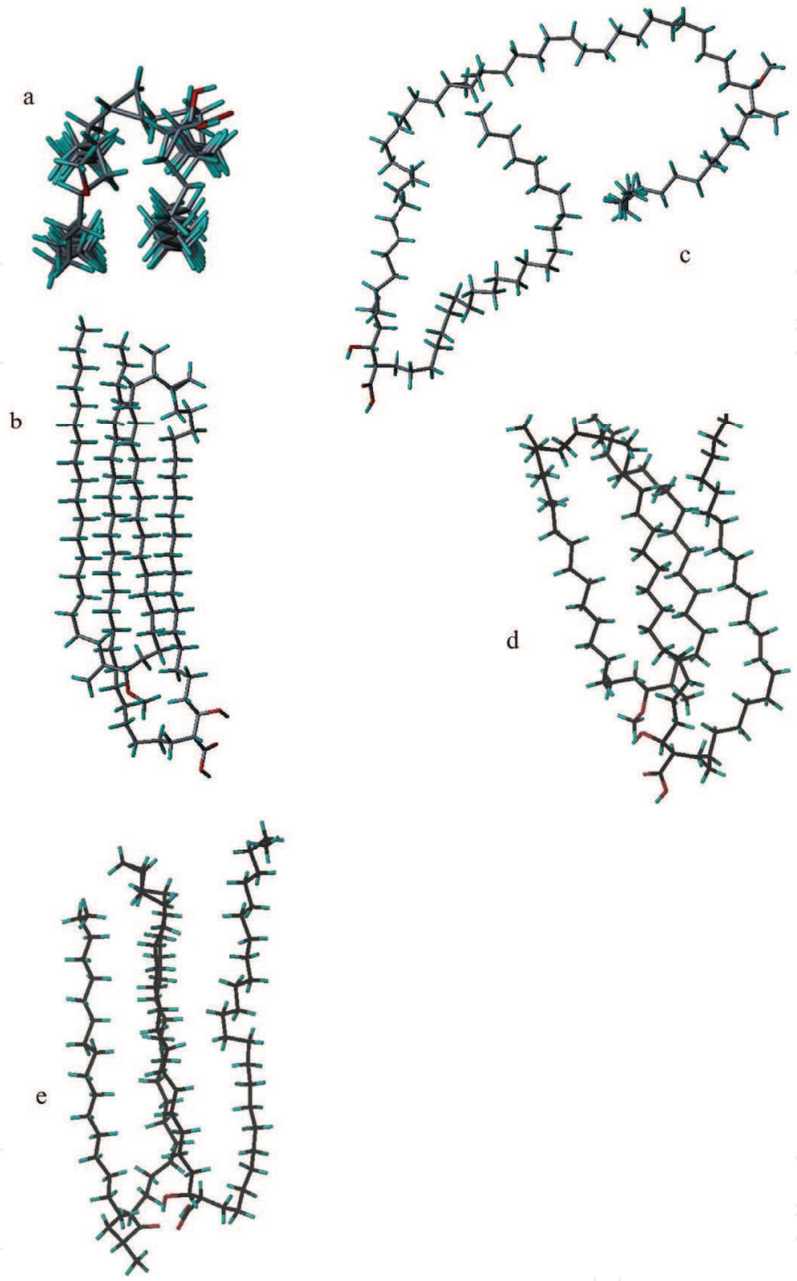

Fig. 10. Structures of MAs in MD study. (a) and (b) Top and side views of MeO-MA molecule obtained by MC followed by minimization; (c) MeO-MA taking a stretched-out structure after 20 ps in MD; (d) MeO-MA retaining a 4-cain structure after 20 ps in MD; (e) structure of Keto-MA obtained after 20 ps in MD.

6. A tentative interpretation of the model membrane in terms of biological activity

6.1 Generality

In relating the present results to the biological role of mycolic acids, the most valuable finding is the special behavior of the Keto-MA. It has exceptional rigidity in monolayers, over a

wide temperature range (Fig. 7), apparently assuming a W-shaped conformation with four hydrocarbon chains packing together in parallel. To our knowledge, this is the first time that fatty acid packing of this type has been detected in nature. The initial studies (Minnikin & Polgar, 1967, 1; 2) on the location of functional groups in cyclopropyl MA showed that these fatty acids are assembled according to a generalized template, with groups spaced at regular intervals separated by relatively uniform lengths of hydrocarbon chains (Table 1); these results have been thoroughly substantiated in recent studies (Watanabe et al., 2001; 2002). The current results offer the first justification for this exquisite regular architecture of mycobacterial MAs. The true reason for the presence of oxygenated functions in MAs is also revealed as being necessary for conformational stabilization probably through hydrophilic interactions. In this model monolayer study, the hydrophilic interaction is most likely to be with the aqueous sub-phase. In the cell envelope of mycobacteria, however, the interaction of the keto group could either be with the covalently attached arabinogalactan or, more intriguingly, with the mycolic acid 3-hydroxy group. This latter interaction could take place in an inter- or intramolecular fashion.

Biological activities of living cells rely upon, not only the relevant chemical reactions but also on relating physicochemical or physical processes. In this study, we have shown that MAs of different chemical structures form Langmuir monolayers having distinctive physicochemical features and each MA exhibits multiple phase transitions depending upon the temperature and the surface pressure. Dubnau (Dubnau et al., 2000) et al. reported that in a *M. tb* strain whose cell wall-linked mycolate consists solely of α-MA, the permeation rate was very low, and Yuan et al. (Yuan et al., 1998) reported that in a recombinant mycobacterial strain whose Keto-MA is completely replaced by MeO-MA showed poor growth in macrophages and a decreased rate of permeation for hydrophilic substances. Those studies imply that different mycolates in the cell envelope contribute differently to the permeability function of the mycolate layer of the cell envelope. It seems possible that each component mycolate takes different conformation in the cell envelope mycolate layer as suggested by the present study, and that the different forms of different mycolates have different effects on the cell function, though we should be careful in applying the monolayer results to the natural cell wall mycolate layer functions.

6.2 Roles of α-MAs

Recent papers revealed better defined features of the outer membrane lipid bilayer of mycobacterial cells by the cyro-electron tomography (Hoffmann et. al., 2008; Niederweis et al., 2010; Zuber et al., 2008). On the basis of the thickness of the layer, in those papers, the cell-bound MAs constituting the basis of the inner leaflet of the outer membrane lipid bilayer are suggested to be in the W-shape. However, if MAs in the lipid bilayer are to take basically the W-shape, it does not necessarily mean that all the MAs are to stay in the W-shape. In the biological lipid bilayers, at biological temperatures, it is well known that the component molecules are able to move quite easily to shift their locations in the layer or to change the conformation. Our present monolayer studies and computer simulation results showed that the α-MAs are ready to change the conformation from the W-shape to any of the various extended shapes as required or favored by its environment. In the outer membrane lipid layer, α-MAs, a large molecular weight component, may change the conformation to various extended shapes and probably by dynamically waving and bending the variously extended

long hydrocarbon chains, may take an initiative active part in making the lipid layer more mobile and biologically compatible.

The observations of α-MAs, especially of the flexible conformational behavior of the molecules and of various characteristics closely and directly related to the physical nature of the lipid layer may imply importance of the presence of α-MAs always in about 50 % of the whole cell-bound MAs in mycobacterial cells.

6.3 Roles of oxygenated-MAs

The possible special influence of MAs with a *trans*-cyclopropane ring on membrane function or pathogenicity of the cells has been highlighted (Glickman et al., 2000; 2001). When the features of the Langmuir monolayers of MeO- and Keto-MAs from BCG in the present study were compared with those of the corresponding MAs from *M. tb* in our study (Villeneuve et al., 2005), some differences were noted. The collapse pressures of Keto-MA and the surface pressures of MeO-MA at the phase transition from the 4-chain conformation to the extended one were lower in those of Keto- and MeO-MAs from BCG, respectively, than in those from *M. tb*, at all the temperatures assayed. The structures of the molecular components of the MAs from the two mycobacteria are essentially identical and the difference is only in the ratios. The ratios between the *cis*-cyclopropane and *trans*-cyclopropane contents are 1/0.03 and 1/0.22, respectively, in MeO-MAs from BCG and *M. tb* and is 1/0.33 and 1/3.5, respectively, in Keto-MAs from BCG and *M. tb*. The differences noted in the respective phase diagrams or isotherms may be attributed to subtle differences in the properties of the *cis*-cyclopropane rings and the *trans*-cyclopropane rings with an adjacent methyl branch. Apparently an increased ratio of *trans*-isomers seems to stabilize the four-chain conformation of the oxygenated MAs. The MD studies did not demonstrate any clear difference between the conformational behaviors of *cis*-cyclopropane-containing and *trans*-cyclopropane-containing MAs. This confirms the previous conclusion (Villeneuve et al., 2005) that *trans*-cyclopropane units, with an adjacent methyl branch, are able to allow folding of MAs in a similar manner to that allowed by *cis*-cyclopropane rings. Further studies on individual molecular species of oxygenated mycolates should be of great value to clear this problem.

Many factors are involved in the process of the onset of infectious diseases. In the case of tuberculosis, the primary and characteristic factor relating to the onset of the disease should be the intrinsic capacity of the *M. tb* cells to resist and reject the attacks by the defense mechanisms of human host cells. If the mycolate layer of the cell envelope is to play a determining role in the permeability barrier function, as suggested (Minnikin, 1982; Puech et al., 2001; Rastogi, 1991), then the layer is to take an active part in regulating the in and out passages of essential factors vital for the living bacteria and thus to control the viability of the bacterial cells. The component MAs, therefore, may be considered to be responsible for the viability of the *M. tb* cells in human cells and detailed analysis of the physicochemical features of the component MAs may help to clear part of the problems relating to the human tuberculosis.

MAs from pathogenic *M. tb* and from non-pathogenic BCG are the same in the chemical structures of each component and slightly different in the ratios between the *trans*-cyclopropane-containing and *cis*-cyclopropane-containing components. One marked difference between the MAs from the two is in the ratios between the non-oxygenated MA (alpha-MA) and the oxygenated MAs. The ratio in the former is roughly 1:1, whereas that

in BCG reaches 1:3.5, in which the oxygenated MA is often mostly Keto-MA (Watanabe et al., 2001). The actual surface pressure in the cell envelope mycolate layer is unknown, but whatever the environmental conditions may be, as demonstrated in the present study, Keto-MAs form compact, relatively solid domains with a minimum thickness in the mycolate monolayer. Such Keto-MA units may provide a relatively impermeable stable foundation in the outer leaflet of the cell envelope. A larger number of, or a larger proportion of this type of less permeable compact domains in BCG cell envelope may provide the cells with the features that distinguish BCG cells from *M. tb* cells. The presence of such solid domains may provide BCG cells with slower and lower multiplication rate and fairly good or moderate resistance to the killing system of the host cells so that the cells can survive quietly for a long time, which is an essential and necessary requirement for a good live vaccine.

The extended structures of MeO-MA, produced by MD simulation, are not of two long straight methylene chains. As exemplified in Fig. 1c, the long chains curve and bend, implying that they are ready to change their conformation in response to the environmental conditions. Probably MeO-MA and also alpha-MA are to be considered to provide less condensed organelles suitable for facilitating selective permeability and interaction with complex cell surface free lipids.

7. References

Al Dulayymi, J. R., Baird, M. S., Roberts, E. (2005), The synthesis of a single enantiomer of a major α-mycolic acid of *M. tuberculosis*, *Tetrahedron* Vol. 6, pp. 11939-11951.

Asselineau, C. & Asselineau, J. (1966), Stéréochimique de l'acide corynomycolique, *Bull. Soc. Chim. France* pp. 1992-1999.

Jackson, M., Raynaud, C., Lanèelle, M.-A., Guilhot, C., Laurent-Winter, C., Ensergueix, D., Gicquel, B., Daffé, M. (1999), Inactivation of the antigen 85C gene profoundly affects the mycolate content and alters the permeability of the *mycobacterium tuberculosis* cell envelope, *Mol. Microbiol.* Vol. 31, pp. 1573-1587.

Dubnau, E., Chan, J., Raynaud, C., Mohan, V. P., Lanèelle, M.-A., Yu, K., Quémard, A., Smith, I., Daffée, M., (2000), Oxygenated mycolic acids are necessary for virulence of *Mycobacterium tuberculosis* in mice, *Mol. Microbiol.* Vol. 36, pp. 630-637.

Glickman, M. S., Cox, J. S., Jacobs Jr., W. R., (2000), A novel mycolic acid cyclopropane synthetase is required for cording, persistence and virulence of *Mycobacterium tuberculosis*, *Mol. Cell* Vol. 5, pp. 717-727.

Glickman, M. S., Cahill, S. M., Jacobs Jr., W. R. (2001), The *Mycobacterium tuberculosis cmaA2* gene encodes a mycolic acid *trans*-cyclopropane synthetase, *J. Biol. Chem.* Vol. 276, pp. 2228-2233.

Goren, M. B. & Brennan, P. J. (1979), Mycobacterial lipids: Chemistry and biologic activities, In: *Tuberculosis*, Youmans, G.P. (Ed.), page numbers (first-last), Saunders, ISBN, Philadelphia.

Hasegawa, T., Nishijo, J., Watanabe, M., Funayama, K., Imae, T. (2000), Conformational characterization of a-mycolic acid in a monolayer film by the Langmuir-Blodgett technique and atomic force microscopy, *Langmuir* Vol. 16, pp. 7325-7330.

Hasegawa, T., Nishijo, J., Watanabe, M., Umemura, J., Ma, Y., Sui, G., Huo, Q., Leblanc, R. M. (2002), Characteristics of long-chain fatty acid monolayers studied by infrared external-reflection spectroscopy, *Langmuir* Vol. 18, pp. 4758-4764.

Hasegawa, T. & Leblanc, R. M. (2003), Aggregation properties of mycolic acid molecules in monolayer films: a comparative study of compounds from various acid-fast bacterial species *Biochim. Biophys. Acta* Vol. 1617, pp. 89-95.

Hasegawa, T., Amino, S. Kitamura, S., Matsumoto, R., Katada, S., Nishijo, J. (2003), Study of the molecular conformation of α- and keto-mycolic acid monolayers by the Langmuir-Blodgett technique and Fourier transform infrared reflection-adsorption spectroscopy, *Langmuir* Vol. 19, pp. 105-109.

Hoffmann, C., Leis, A., Niederweis, M., Plitzko, J. M., Engelhardt, H. (2008), Disclosure of the mycobacterial outer membrane: Cryo-electron tomography and vitreous sections reveal the lipid bilayer structure, *PNAS* Vol. 105, pp. 3963-3967.

Hong, X. & Hopfinger, A. J. (2004), Construction, molecular modeling, and simulation of *mycobacterium tuberculosis* cell walls, *Biomacromolecules* Vol. 5, pp. 1052-1065.

Motomura, K. (1967), Thermodynamics and phase transitions in monolayers, *J.C.I.S.* Vol. 23, pp. 313-318.

M. McNeil, M. Daffé, P. J. Brennan (1991), Location of the mycolyl ester substituents in the cell walls of mycobacteria, *J. Biol. Chem.* Vol. 266, pp. 13217-13223.

Minnikin, D. E. & Polgar, N. (1967), The mycolic acids from human and avian tubercle bacilli, *Chem. Comm.* pp. 916-918.

Minnikin, D. E. & Polgar, N. (1967), The mycolic acids from human and avian tubercle bacilli, *Chem. Comm.* pp. 1172-1174.

D. E. Minnikin (1982). Lipids: Complex Lipids, Their Chemistry, Biosynthesis and Roles, In: *The Biology of the Mycobacteria Vol. 1*, Ratledge, C. & Stanford, J. L. (Ed.), pp. 95-184, Academic Press, New York.

Minnikin, D. E., Kremer, L., Dover, L. G., Besra, G. S. (2002), The methyl-branched fortifications of Mycobacterium tuberculosis, *Chem. Biol.* Vol. 9, pp. 545-553.

Niederweis, M., Danielchanka, O., Huff, J., Hoffmann, C., Engelhardt, H. (2010), Mycobacterial outer membranes: in search of proteins, *Trends in Microbiology* Vol. 18, pp. 109-116.

Puech, V., Chami, M., Lemassu, A., Lanèelle, M.-A., Schiffler, B., Gounon, P., Bayan, N., Benz, R., Daffé, M. (2001), Structure of the cell envelope of corynebacteria: importance of the non-covalently bound lipids in the formation of the cell wall permeability barrier and fracture plane, *Microbiology* Vol. 147, pp. 1356-1382.

Rastogi, N. (1991), Recent observations concerning structure and function relationships in the mycobacterial cell envelope: elaboration of a model in terms of mycobacterial pathogenicity, virulence and drug-resistance, *Res. Microbiol.* Vol. 142, pp. 464-476.

Staellberg-Stenhagen, S. & Stenhagen, E. (1945) A monolayer and X-ray studies of mycolic acid from the human tubercle bacillus, *J. B. C.* Vol. 150, pp. 255-262.

Timmons, C. O. & Zisman, W. A. (1968) The relation of initial spreading pressure of polar compounds on water to interfacial tension, work of adhesion, and solubility, *J.C.I.S.* Vol. 28, pp. 106-117.

Tocanne, J. F. & Asselineau, C. (1968), Étude stéréochimique des acides aliphatiques α-ramifiés β-hydroxylés. Configuration de l'acide corynomycolique, *Bull. Soc. Chim. Fr.* pp. 4519-4525.

Tompkins, H. G. & McGahan, W. A. (1999). *Spectroscopic Ellipsometry and Reflectometry: A User's Guide*, Wiley-Interscience, New York.

Villeneuve, M. Kawai, M., Kanashima, H., Watanabe, M., Minnikin, D. E., Nakahara, H. (2005), Temperature dependence of the Langmuir monolayer packing of mycolic acids from *Mycobacterium tuberculosis*, *Biochim. Biophys. Acta* Vol. 1715, pp. 71-80.

Villeneuve, M. Kawai, M., Watanabe, M., Aoyagi, Y., Hitotsuyanagi, Y., Takeya, K., Gouda, H., Hirono, S., Minnikin, D. E., Nakahara, H. (2007), Conformational behavior of oxygenated mycobacterial mycolic acids from *Mycobacterium bovis* BCG, *Biochim. Biophys. Acta* Vol. 1768, pp. 1717-1726.

Villeneuve, M. Kawai, M., Watanabe, M., Aoyagi, Y., Hitotsuyanagi, Y., Takeya, K., Gouda, H., Hirono, S., Minnikin, D. E., Nakahara, H. (2010), Differential conformational behavior of *α*-mycolic acids in Langmuir monolayers and computer simulations, *Chemistry and Physics of Lipids* Vol. 163, pp. 569-579.

Watanabe, M., Aoyagi, Y. Ridell, M. Minnikin, D. E. (2001), Separation and characterization of individual mycolic acids in representative mycobacteria, *Microbiology* Vol. 147, pp. 1825-1837.

Watanabe, M., Aoyagi, Y. , Mitome, H. ,Fujita, T., Naoki, H., Ridell, M., Minnikin, D. E. (2002), Location of functional groups in mycobacterial meromycolate chains; the recognition of new structural principles in mycolic acids, *Microbiology* Vol. 148, pp. 1881-1902.

Yuan, Y., Zhu, Y. Q., Crane, D. D., Barry III, C. E. (1998), The effect of oxygenated mycolic acid composition on cell wall function and macrophage growth in *mycobacterium tuberculosis*, *Mol. Microbiol.* Vol. 29, pp. 1449-1458.

Zuber, B., Chami, M., Houssin, C., Dubochet, J., Griffiths, G., Daffé, M. (2008), Direct visualization of the outer membrane of mycobacteria and corynebacteria in their native state, *Journal of Bacteriology* Vol. 190, 5672-5680.

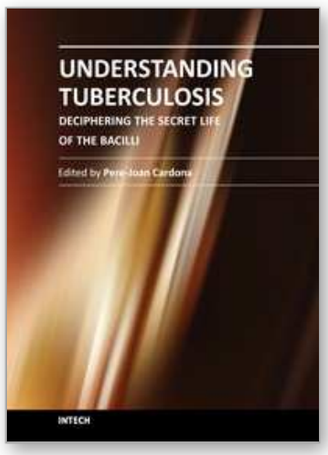

Understanding Tuberculosis - Deciphering the Secret Life of the Bacilli

Edited by Dr. Pere-Joan Cardona

ISBN 978-953-307-946-2
Hard cover, 334 pages
Publisher InTech
Published online 17, February, 2012
Published in print edition February, 2012

Mycobacterium tuberculosis, as recent investigations demonstrate, has a complex signaling expression, which allows its close interaction with the environment and one of its most renowned properties: the ability to persist for long periods of time under a non-replicative status. Although this skill is well characterized in other bacteria, the intrinsically very slow growth rate of Mycobium tuberculosis, together with a very thick and complex cell wall, makes this pathogen specially adapted to the stress that could be generated by the host against them. In this book, different aspects of these properties are displayed by specialists in the field.

INTECH
open science | open minds

InTech Europe
University Campus STeP Ri
Slavka Krautzeka 83/A
51000 Rijeka, Croatia
Phone: +385 (51) 770 447
Fax: +385 (51) 686 166
www.intechopen.com

InTech China
Unit 405, Office Block, Hotel Equatorial Shanghai
No.65, Yan An Road (West), Shanghai, 200040, China
中国上海市延安西路65号上海国际贵都大饭店办公楼405单元
Phone: +86-21-62489820
Fax: +86-21-62489821

IntechOpen